UNIVERSITY OF CALIFORNIA
RIVERSIDE

Induction of Ileal Microfold Cells Produced by Cholera Toxin Enhances Bacterial Adherence

A Thesis submitted in partial satisfaction of the
requirements for the degree of

Masters of Science

in

Bioengineering

by

Candice April Sanscartier

June 2016

Thesis Committee:
Dr. David D. Lo, Chairperson
Dr. Victor G. J. Rodgers
Dr. Sharon Walker

The Thesis of Candice April Sanscartier is approved:

_____

_____

_____

Committee Chairperson

University of California, Riverside

Acknowledgements

First and foremost, I would like to express immense gratitude for my advisor and committee chair Dr. David D. Lo for his guidance, patience, and support throughout the completion of my Masters degree. I appreciate his ample supply of knowledge and endless giving nature towards this thesis and my graduate work. It has been a pleasure and honor to work with him.

I would also like to acknowledge and express my gratitude to my committee members Dr. Victor Rodgers and Dr. Sharon Walker for their immeasurable guidance toward the completion of my thesis. Dr. Rodgers has provided endless supported throughout my graduate career with guidance, recommendations and completion to this thesis, his personal assistance helped me overcome obstacles during my graduate studies and he is a significant reason I pursued the path of a graduate degree. Dr. Sharon walker has given invaluable suggestions and knowledge contributing to this thesis and my professional career.

I am also indebted too and want to acknowledge the help from fellow colleagues Dr. Erinn Parnell and Dr. Olivia Sakhon. Both have offered infinite encouragement, comfort, kindheartedness and knowledge, which helped me endure and get through my graduate studies. I am eternally grateful for their guidance, friendship and accompaniment on this journey. I would also like to acknowledge the help of the many undergraduates whom where part of our team in helping complete the experiments, collecting the data and contributing to the analytical components for this thesis. I want to acknowledge former

graduate students for their initiation and development to the project without whom this work would not be as substantial or significant.

I would like to recognize my funding sources for providing education and research support, the Deans funding from the bioengineering department and my GSR funding through my advisor Dr. Lo.

An enormous amount of this work would not be done without the facilities used to obtain images and analyses in this thesis. I thank the center facility for advanced microscopy and microanalysis (CFAMM) at the University of California, Riverside for providing preparation equipment, scanning electron microscope, and advice on making the images pristine. I also want to thank the microscopy team at City of Hope (COH) for processing and imaging intestinal samples with the transmission electron microscope.

Finally, I must express my profound gratitude towards my parents Paul and Lillian Sanscartier whom have supported me every step of the way. They have been there when experiments didn't go accordingly, through my many stages of stress, and rushing to meet all deadlines. They have given me strength and motivation to pursue my dreams and overcome obstacles I didn't think were possible. This endeavor would not have been possible without the love and counsel they have provided throughout my life.

ABSTRACT OF THE THESIS

Induction of Ileal Microfold Cells Produced by Cholera Toxin Enhances Bacterial Adherence

by

Candice April Sanscartier

Masters of Science, Graduate Program in Bioengineering
University of California, Riverside, June 2016
Dr. David D. Lo, Chairperson

Microfold (M) cells are a type of epithelial cell specialized for antigen uptake and are present within many mucosal associated lymphoid tissues (MALT). These M cells vary in different MALT tissues with regard to their surface receptors, apical morphology, and function. In the small intestine, M cells are found more abundantly in the distal portion than in the proximal portion. In the presence of cholera toxin (CT), a bacterial toxin secreted from *Vibrio cholerae*, M cell clusters are induced on villous tips 48 hours post-administration. This study has determined that CT-induced M cell clusters are phenotypically different from other intestinal M cells and allow for greater bacterial adherence. This is potentially due to their absence or the reorganization of microvilli, which in theory disperses and/or lowers the electrostatic repulsion towards luminal microparticles. We see similar microvilli effacement in *in vitro* Caco2 BBe cultures, where cells treated with CT produce bare apical surfaces. This is not an effect from glycoprotein linkage depletion, which would affect microvilli structure. It remains to be determined whether the M cell clustering and microvilli effacement are more beneficial to the host,

for immunosurveillance, or invading pathogens that take advantage of the apical change for colonization. These phenotypic changes could be utilized for rationally targeting therapeutics for uptake by M cells.

Table of Contents

List of Figures

Chapter 1 – Introduction

Understanding host-pathogen interactions is a key aspect for understanding diseases, infections, etc., and how our immune system reacts. The system we are studying are mucosal tissues; specifically, the interaction between intestinal epithelial cells and cholera toxin (CT) secreted by the bacterium *Vibrio cholerae.* A significant characteristic of microfold (M) cells is the ability to bind and sample microparticles in the intestinal lumen, therefore our focus is to elucidate the interactions between CT and intestinal epithelial M cells.

Mucosal Immunology

Mucosal immunology studies focus on the protection, interaction and response to microbes and foreign particles within mucosal tissues. These mucosal tissues include bronchus-associated lymphoid tissue (BALT) and nasal-associated lymphoid tissue (NALT) of the respiratory tract, and the gut-associated lymphoid tissue (GALT) of the gastrointestinal and urogenital tracts. Each is composed of a complex network between the tissue barrier, migratory or resident immune cells, and commensal microorganisms. Our main focus is on the gastrointestinal tract, specifically the small intestine, which is internally lined by finger-like protrusions called villi. The epithelium lines the apical surface of the tissue-lumen interface and is composed of a single layer of columnar epithelial cells that help maintain homeostasis within the system allowing interaction and

communication between antigen presenting cells (APCs) of self or foreign antigens. These epithelial cells originate from stem cells in the crypts between villi, which migrate to the tips of the villi where they slough off after a lifespan of four to six days (Ross et al. 2003; Van der Flier et al. 2009). A subset of cells in the epithelium includes enterocytes, goblet cells, and M cells.

Enterocytes

Enterocytes have a distinct apical surface of micron-sized membrane protrusions, called microvilli, composed of actin filaments and glycoproteins for structural support. Enterocytes specialize in the exchange of nutrients and ions through channels and transporters located on the microvilli (Lange 2000; Ross et al. 2003). When fully mature, these microvilli form transmembrane glycoprotein linkages between neighboring microvilli that aid in establishing and maintaining upright microvilli, creating a tightly packed brush border (BB) that makes invasion difficult. The glycoprotein linkages involve two transmembrane proteins; protocadherin-24 (PCDH24) and mucin-like protocadherin (MLPCDH) (Crawley et al. 2014). Crawley et al. (2014) demonstrated that without the glycoprotein linkages between PCDH24 and MLPCDH microvilli fold over. Not only are microvilli crosslinked with glycoproteins, but the majority of their composition is derived of glycoproteins. Since glycoproteins are negatively charged, the microvilli are also believed to provide a powerful electrostatic force (Bennett et al. 2014), possibly acting as a protective barrier against pathogens, for blocking and guiding microorganisms to more neutrally charged M cells.

Goblet cells

Another cell type contributing to the protection of mucosal surfaces are goblet cells. These cells secrete mucus, which is composed of a glycocalyx matrix that varies in thickness along the gastrointestinal tract. Mucus is thickest in the distal section of the small intestine, the ileum, and in the colon (Atuma et al. 2001). The thick matrix protects the epithelium from foreign microparticles while also providing an environment for endogenous microflora. Mucus is produced in two layers; a larger loosely adherent layer and a thin firmly adherent layer (Atuma et al. 2001). Goblet cells are constantly renewing the mucus to rid the environment of microorganisms that become trapped in the loosely adherent layer. It is suggested that the amount of mucus in the small intestine and colon is proportionally associated with the populations and species of bacteria (Mowat et al. 2014). While goblet cells are great protectors to the epithelial barrier we want to address the effects and properties other epithelial cells establish when they interact with pathogenic bacteria.

M cells

The epithelium contains specialized cells, M cells, which survey luminal antigens through uptake of microparticles and interaction with various APCs and lymphocytes. M cells are found throughout mucosal tissues, however, my research focuses on the small intestine with little emphasis on the colon. M cells found on these surfaces include villous M cells, Peyer's patch (PP) follicle associated epithelial M cells, and colonic M cells. Although these M cells may show similar function, they express different surface markers

allowing them to recognize various antigens. A variety of receptors and markers have been identified for M cells located in the gastrointestinal tract and can be found in Table 1.1 (Clark et al. 1993; Hase et al. 2009; Wang et al. 2011; Hsieh et al. 2010; Peterson et al. 2014). The most commonly used markers used to identify M cells include: (1) the lectin *Ulex europeus* agglutinin-1 (UEA-1) that binds fucose, specifically α-1,2 fucosylation sites, on M cells; (2) glycoprotein 2 (GP2), a receptor on M cells which interacts with FimH on type I pilus gram negative bacteria; and (3) peptidoglycan recognition protein-short (PGRP-S), another receptor on M cells that recognizes a variety of pathogen-associated molecular patterns. It has been suggested that the differentiation into the various types of intestinal M cells and associated gene expression may be influenced by Notch signaling (Hsieh et al. 2012). These receptors or marker recognition sites, as well as signaling pathways, may contribute to the diversity of intestinal M cells.

Diseases Associated with Increased M Cell Populations

M cells are vital for sampling the environment and transporting microparticles across the epithelial barrier for an immune response to then be initiated. Others have noted a change in epithelium plasticity in the presence of some bacteria, which causes an induction of M cells. A few of these include *Vibrio cholerae, Salmonella Typhimurium,* and *Streptococcus pneumoniae* R36a (Wang et al. 2011; Savidge et al. 1991; Borghesi et al. 1999, Meynellet al. 1999) however, in some cases it is uncertain if this is a host-initiated or bacteria-initiated response.

A disease associated with an induction of M cells that our lab has particular interest in is colitis. Bennett et al. (2016) showed an induction of colonic M cells in two colitis models; seven days of dextran sodium sulfate treatment and six days of *Citrobacter rodentium* infection. The colitis disease model requires approximately a week to establish the disease, whereas the lifespan of M cells are four to six days, meaning, colonic induced M cells could originate from differentiating crypt cells.

As mentioned, site-specific M cells have different markers and receptors, which detect different antigens that allow for foreign microparticles to gain access to underlying tissue. In order to understand this host-pathogen interaction and M cell function, we used a model in which we administer CT to induce M cells. Cholera is caused by infection with the bacterium *Vibrio cholerae* and its type II secretion of CT. CT is internalized into the host cell, adheres to the G protein, $G_{s\alpha}$, causing ADP ribosylation resulting in excess production of cyclic AMP and chloride ion efflux leading to diarrhea (Lencer et al. 2001). Wang et al. (2011) demonstrated an induction of sporadic M cells in PPs and clusters on small intestine villi in as little as 48 hours post-CT administration. A major distinction between CT-induced M cells and colitis-induced M cells is the time frame of induction. The life span of epithelial cells from the crypt to the villous tip is 4-6 days (Ross et al. 2003; Van der Flier et al. 2009), which means it is less likely CT-induced villous M cells could be produced through normal crypt cell differentiation.

The reason why these M cells are induced in specific regions is less known. It is vital to understand the function of these induced M cells and if they are beneficial or detrimental to the host during the development and recovery from disease. In this thesis,

we hypothesize that the CT-induced villous M cell clusters are closely related to the endogenous villous M cells in that they aid in host protection by displaying similar surface markers, morphological appearances, and host-pathogen interactions.

	Villous M cells	PP M cells	Colonic M cells
UEA-1	Yes	Yes	No
PGRP-S	No	Yes	Yes
GP2	Yes (variable)	Yes	Yes
Annexin V	Yes	Yes	Unknown
Marcksl1	Yes	Yes	Unknown
Vimentin	No	Unknown	Yes
PrP^C	Unknown	Yes	Unknown

Table 1.1 Summary of the surface receptors and recognizable markers on various types of gastrointestinal M cells. Surface markers are located in the left column and the M cell types are located on the top row. If the marker is present in that M cell type it is marked with a Yes, if it is not present it has a No, if the surface marker is not known it is marked with an Unknown. The three main M cell markers are *Ulex europeus* agglutinin-1 (UEA-1), peptidoglycan recognition protein-short (PGRP-S), and glycoprotein 2 (GP2). While GP2 is present on all populations literature suggest it inconsistently stains all M cells in a particular population. PGRP-S and UEA-1 are other common markers however; PGRP-S is not present in villous M cells but present in colonic M cells while UEA-1 is opposite of this. We focus our research on villous M cells therefore, UEA-1 is the best marker for these M cells.

Chapter 2 – Materials and Methods

In this thesis, we examined the induction of M cells via CT and its comparison to endogenous M cells by small intestine location, morphological characteristics and bacterial adherence properties. We analyzed the similarities and differences between the two populations and provide information on the induced M cells and their role associated on mucosal surfaces *in vivo*. We also analyzed enterocyte microvilli effacement caused by CT, *in vitro*. To evaluate such properties, we utilized electron micrographs for aerial and cross-sectional views, fluorescent images for bacterial adherence assays and microvilli effacement profiles, and statistical analyses to evaluate data.

Animals

C57BL/6 mice (Jax #0664, Jackson Laboratories, Sacramento, CA) were bred in the University of California, Riverside vivarium facilities following specific pathogen-free conditions. Mice were used between 8 to 16 weeks of age and were handled following IACUC and NIH guidelines.

Cell culture

C2BBe1 cells (clone of Caco-2, Caco2BBe, ATCC® CRL-2102, Manassas, VA) were grown for 3 weeks to form mature cell polarization in Advanced Dulbecco's Modified Eagle's Medium (12-491-023, ADMEM, Thermo Fisher, Waltham, MA). Media

was supplemented with 10% fetal bovine serum (S1520, Biowest, Riverside, MO), 1% 4-(2-hydroxyethyl)-1-piperazineethanesulfonic acid (HEPES) (Cellgro® Mediatech, Manassas, VA), and 1% penicillin-streptomycin-glutamine (Cellgro® Mediatech, Manassas, VA). Cells were seeded in 35 mm collagen-coated glass bottom dishes (MatTek Corporation, Ashland, MA) at a seeding density of 400,000 cells per dish and media was changed every three days.

Cholera toxin administration

Cholera toxin (100B, List laboratories, Campbell, CA) was reconstituted in phosphate buffered saline (PBS) (Fisher Scientific, Waltham, MA) to a final concentration of 1 µg/µl. A 10 µg dose was administered into each mouse by intraperitoneal injection (in 200 µl 1x PBS). Approximately 48 hours post-administration, mice were euthanized and organs were harvested for analysis.

Scanning electron microscopy and M cell counts

Small intestines were fixed with 2.5% glutaraldehyde (GA) solution (Electron Microscope Sciences, Hatfield, PA) for two hours. Samples were washed three times for 10 minutes each with PBS (Fisher Scientific, Waltham, MA), then 1% osmium tetroxide (Sigma Aldrich, St. Louis, MO) was added for three hours. Samples were washed again with as described above then gradually dehydrated in 25, 50, 75, 90, and 100% ethanol in 10 minute intervals. Dehydrated samples remained immersed in 100% ethanol. Critical-

point drying was performed by using a critical-point dryer (Autosamdri®-815 series B, Tousimis, Rockville, MD). Samples were then mounted onto pin stub mounts (Ted Pella, Redding, CA) with carbon-coated conductive tape, and finally, sputter coated with platinum/palladium for 60-75 seconds (Cressington 108 Auto sputter coater, Watford, UK). The samples were viewed by scanning electron microscope (SEM) (FEI XL-30 FEG, FEI, Hillsboro, OG) at 5 kV.

Transmission electron microscopy

Small intestines were fixed in a solution containing 2.5% GA (Electron Microscope Sciences, Hatfield, PA), 2% paraformaldehyde (PFA) (Alfa Aesar, Ward Hill, MA), 0.15 M cacodylate buffer (Electron Microscope Sciences, Hatfield, PA), and 2 mM calcium chloride. Tissue resided in fixative solution until it reached its destination and then was ready to be processed. Samples were sent to City of Hope (Duarte, CA) to be further fixed using the osmium tetroxide method, and analyzed using transmission electron microscopy (TEM) (Tecnai^{TM} 12, FEI, Hillsboro, OR).

Immunofluorescence imaging

Ileum and duodenum sections were placed in 4% PFA (Electron Microscopy Sciences, Hatfield, PA) and 30% sucrose/PBS (Fisher Scientific, Waltham, MA) solution for two hours. Fixed tissues were cut into approximately 2 mm sections and frozen in optimal cutting temperature (OCT) embedding medium (Sakura, Torrance, CA). Tissue

sections were cut using a Cryostat (CM1850, Leica Biosystems, Buffalo Grove, IL). Cryostat sections were treated with 0.5% Tween-20 (Fisher scientific, Waltham, MA) in PBS (Fisher Scientific, Waltham, MA), washed three times in 0.1%Tween/PBS and then blocked using 0.1% Tween-20 in casein solution (ThermoFisher Scientific, Grand Island, NY). Rhodamine-conjugated *Ulex Europeus* Agglutinin 1 (Vector Labs, Burlingame, CA) and rabbit anti-human CDHR2 (Sigma Aldrich, St. Louis, MO) were added to the blocking solution, incubated and washed. Secondary Phalloidin Alexa Fluor® 568 (Molecular Probes™, Waltham, MA), and goat anti-rabbit Alexa Fluor® 488 (Life Technologies, Waltham, MA) were added. Tissue was again washed and mounted with ProLong® Gold Antifade Reagent (Life Technologies, Waltham, MA) containing DAPI (4′,6-diamidino-2-phenylindole). Images were obtained by using a spinning disk confocal imager (CarvII, BD Biosystems, San Jose, CA) attached to a Zeiss Axio Observer inverted microscope. Hardware, including the confocal microscope and digital camera (Qimaging® Rolera™ EM-C^2, BC, Canada), was controlled by imaging software (Metamorph® version 7.7.9.0, Molecular Devices, Sunnyvale, CA). Images were analyzed by using imaging software (Volocity® version 6.1.1 PerkinElmer, Waltham, MA).

Bacteria culture and intestinal uptake

Green fluorescent protein (GFP)-labeled *Staphylococcus aureus* cultures were grown in LB broth (Fisher Scientific, Waltham, MA) under erythromycin selection (Fisher Scientific, Waltham, MA), shaking at 250 rpm at 37°C for a minimum of 12 hours. After

the incubation period, the bacteria were pelleted, washed twice, and re-suspended for counting. The concentration was adjusted to obtain 1 x 10^9 bacteria per 200 µl. Mice were anesthetized with 2,2,2,-tribromoethanol (Sigma Aldrich, St. Louis, MO) diluted in PBS. A one centimeter abdominal midline incision was made into the peritoneal cavity and the ileum was isolated. Five to seven centimeters of the ileum was ligated with surgical thread, injected with the bacteria, and incubated for 15 minute time periods. Mice were sacrificed and the ligated ileum was collected and fixed in 4% PFA and 30% sucrose in 1x PBS solution for two hours. Samples were cut into approximately 2 mm long sections and frozen in OCT. Samples were cryosectioned using the cryostat (CM1850, Leica Biosystems, Buffalo Grove, IL) and imaged using confocal microscope. Images were taken of villous tips containing UEA-1^+ M cells. Bacterial quantification was performed using software (Volocity® version 6.1.1, PerkinElmer, Waltham, MA).

Volocity® imaging processing

Volocity®, fluorescent imaging processing software, was used to count the amount of objects defined as bacterial cells, isolated cells, and clustered cells. Using object recognition and standard size input parameters of cells and bacteria, the amount of adhered bacteria per isolated and clustered M cells was determined. Bacteria were identified using the find objects tools within the measurements area. This object was labeled bacteria and recognized objects with a diameter size of 1-2 µm of the GFP channel. M cells, isolated and clustered, were identified using a free hand tracing tool on the red fluorescent channel and labeled as the object region of interest. M cell region of interest were length (µm) along

the villi. Bacterial objects, pertaining to adherence to M cells, were identified by using co-localization in the object tool. Bacteria co-localized in the M cell region of interest displayed overlapping of the green and red channels to show yellow. Volocity® software analyzed the amount of bacteria adhered to M cells. The amount of adhered bacteria to isolated and clustered M cell length was calculated per villi. The adhered bacteria calculations were normalized for 100 µm length of isolated and clustered M cells and adherence, if any, to enterocytes of 100 µm length. The length of 100 µm was chosen to have whole numbers of bacteria.

Quantification of in vivo SEM images

M cell counts for optimizing the CT dose and the induced M cell clusters were quantified by capturing SEM images of the small intestine. Cohorts with mice, n=3, were used for these experiments. A total of 25 villi were imaged for the dose optimization and 40 villi for the small intestine M cell location experiment, each at approximately 1000x magnification. The number of M cells, isolated or in clusters, were counted per villous tip.

Quantification of in vitro SEM images

To quantify CT effects on cultured cells, three dishes were seeded per treatment with 10 SEM images captured per dish at a magnification of approximately 2000x. All SEM images were analyzed using the FIJI processing program, an extension of ImageJ. Cell cultures were analyzed to obtain the total area of the cells per image and the area of

bare surfaces per image. Any artifacts of SEM imaging that displayed cracks in cell membranes or obstructions preventing a clear view of the apical surfaces were subtracted from the total area of cells to obtain the true cell area. The percentage was calculated for the amount of bare surfaces of the true cell area.

Quantification of in vivo fluorescent images

For quantifying the amount of bacterial adhesion to CT-induced clusters, we identified the length and number of bacteria adhered to the following classes of cells in both CT and PBS groups: clustered M cells, non-clustered (isolated) M cells, and enterocytes. From the data we normalized the amount of bacteria to cell class by dividing the number of bacteria by length and multiplying to obtain bacteria per 100 μm length.

Statistical analysis

All statistical analysis was performed using software (GraphPad Software version 5.04, La Jolla, CA). All data was input as column (dose optimization, 10 μg dose induction, and *in vitro* cell cultures with CT) or grouped data (*S. aureus* adhesion assay), normalized, and analyzed using unpaired t-tests. All data followed conditions using the Mann-Whitney test for the comparison between control and treated conditions and used a standard error of the mean. Statistical significance was established with a p-value < 0.05.

Chapter 3 – Results

M cell frequency is naturally greater in ileal villous tips and are highly induced with cholera toxin

Intranasal and intraperitoneal CT administration has been shown to induce M cells systemically in mice (Wang et al. 2011). However, it is unknown if there are dose limitations to both the induction and/or the region of highest induction of the small intestine. The dose initially used for stimulating systemic M cell induction was 15 µg CT, therefore we tested the effects of lower doses (5 and 10 µg) and determined both these doses induced M cell clusters on villous tips as seen in Figure 4.1. Interestingly, 5 µg gave a greater induction of M cells, however there was greater variability in the number of M cells induced amongst mice than with the 10 µg dose. The sample size analyzed for these doses were 25 villous tips per intestinal section. This sample size was small compared to the tissue section so we increased the villi sampled to better represent the sample area. The optimal dose to use for induction of M cells clusters, with little variability amongst cohorts, was determined to be 10 µg. This was determined by an analysis showing one mouse in the 5 µg cohort had significantly higher amounts of M cells induced than the other two mice. The 10 µg induced M cells were more evenly distributed amongst the mice in this cohort making it the optimal dose.

The small intestine is composed of three portions, the duodenum, jejunum, and ileum, proximal to distal respectively, and all differ structurally and environmentally. The amount of mucus present in the three sections differs, with the ileum containing about

twice the amount of mucus than in the duodenum (Atuma et al. 2001). With these differences in mind, we examined whether the amount of mucus present contribute to M cell localization in the small intestine.

In our studies, we looked at endogenous M cell location and the effect on M cell populations during CT administration. We sampled a greater amount of villous tips compared to testing the dose optimization, 40 per intestinal section instead of 25, giving a more accurate representation of the tissue. After imaging the three sections (duodenum, jejunum, and ileum) we found little to no villous M cells in the jejunum so for future experiments we only analyzed the duodenum and ileum sections. Our results show endogenous M cells are mainly found in the duodenum and ileum (Figure 4.2). With CT administration, a significantly greater amount of M cells was induced in the ileum over the duodenum with a p-value of 0.0001. There was no significant increase of M cells in the duodenum of the CT-treated mice over the control. Scanning electron images show the difference in M cell populations on ileal villous tips between the untreated and CT-treated mice in Figure 4.3. Untreated mice (Figure 4.3, A) have villi with fewer M cells than the villi in CT-treated mice (Figure 4.3, C). M cells on villi in the untreated and treated mice are magnified to show M cells (Figure 4.3 B and D, respectively). In both conditions, CT-treated and the control, isolated and clustered M cells are seen. However, clusters are much smaller in size in the control villous tips compared to the CT-treated villous tips.

CT induced M cells clusters show similar apical surface phenotypes as endogenous M cells

It is clear that M cell clusters are induced by CT, however these cells exhibit a variety of apical phenotypes, which were identified through transmission electron microscopy (TEM) vertical cross-sectional data (Figure 4.4). Enterocytes are clearly defined by their uniform microvilli BB; however, M cells are known to lack this BB and have thicker apical protrusions. Our TEM data suggests several phenotypes are heightened in CT models including: disorganized microvilli (Figure 4.4 A, E), thicker microvilli (Figure 4.4 B, F), hybrid surfaces half with and half without microvilli (Figure 4.4 C, G), and surfaces without microvilli (Figure 4.4 D, H). The four phenotypes (Figure 4.4 A-D), with the cell of interest outlined with a red dashed line, are each characterized by unique properties which are outlined in magnified images of the apical surface (Figure 4.4 E-H).

Cells displaying disorganized microvilli have areas where microvilli form straight uniform sections and sections where microvilli appear folded over or knotted with neighboring microvilli. Thick microvilli are more consistent with the microfolds on M cell apical surfaces. These surfaces are thicker, approximately 300-600 nm wide (Figure 4.4 F), than the standard 100 nm width of microvilli. Cells exhibiting the half and half properties (Figure 4.4 C) contain areas where the microvilli are extending from the terminal web (tissue between any apical extensions to the cytosol) as well as areas where no microvilli are present (Figure 4.4 G denoted with red box). The last phenotype, bare, presents an apical surface where no microvilli are present (Figure 4.4 D, H). The disorganized phenotype is also more clearly defined by using FIJI software to outline the

prominent characteristics of the microvilli (Figure 4.5). The cell of interest, in the middle, is denoted by the dashed lines. It is clear the microvilli in neighboring cells are in a parallel upright position, whereas the disorganization of the microvilli is shown in the center cell.

All these cells represent characteristics of enterocytes or M cells with their apical surfaces, presence of a terminal web, cross-sectional cytosol components and cell shape. In our observations, endogenous villi have a lower basal level of the four phenotypes discussed above than CT-treated mice. It is important to note the wild type mice very rarely showed the bare surface M cells. To control for non-CT phenomena, we moved our studies to an *in vitro* model to determine if we could replicate our *in vivo* data and if induction of these phenotypes was due to a change in enterocytes apical surface.

Cholera toxin causes microvilli effacement in vitro with Caco2 BBe cells

Our *in vivo* studies suggest that CT induces altered epithelial cell apical phenotypes, therefore we also explored this effect *in vitro*. By using Caco2 BBe enterocytes to demonstrate these phenotypic changes we hypothesized CT would efface the brush border. In order to investigate the effacement, we first established the normal growth stages of microvilli to obtain mature BB before CT administration. Enterocytes line mucosal surfaces protecting these surfaces with tightly packed microvilli. Similarly, cultured Caco2 BBe cells form these borders after adhesion to a surface by first immaturely forming teepee-like structures then maturing into a fully developed BB (Figure 4.6). Other groups have shown the interaction between *Vibrio cholerae* and colon carcinoma epithelial

cells grown *in vitro* (Kerneis et al. 1997) and how CT causes a disruption of tight junction proteins, cortical actin and Notch signaling localization in Caco2 BBe cell cultures (Guichard et al. 2013). We have examined the relationship between microvilli and CT in Caco2 BBe cultures by modifying the administration methods from Guichard et al. 2013.

After reaching culture confluency, we examined the epithelial microvilli effacement by incubating cultures with 1 or 10 µg/mL CT for 6, 24 and 32 hours. We saw little to no effect with either dose at 6 or 24 hours after CT administration. Our results demonstrate that the higher dose at 32 hours is more effective at showing the effacement than the lower dose (Figure 4.7). Images were quantified to determine the proportion of bare apical surfaces induced by CT (Figure 4.8).

Although CT has a substantial effect on the BB, we wanted to look at the mechanism of effacement, by assessing microvilli structure and composition. We hypothesized the effacement is due to intermicrovillar glycoprotein linkage depletion, so we examined PCDH24 after treating with CT. Figure 4.9 illustrates the morphology of a control BB and a BB affected with CT. The BBs exposed to CT have no change in PCDH24 on the tips of their microvilli when compared to control BBs. Since PCDH24 depletion does not seem to be the mechanism in our studies, we could further hypothesize CT affects the microvilli by inhibiting protein synthesis or blocking microvilli proteins from forming such as the ezrin binding complex.

CT-induced M cell clusters have greater amounts of bacterial adherence compared to the endogenous M cells

Bacterial studies *in vivo* are critical for understanding host-pathogen interactions, which in this case is between endogenous or induced M cells and luminal pathogens. M cells are a great asset for sampling micron sized particles via endocytosis. M cells are able to perform this function by surface receptor recognition and it is suggested that enterocytes drive microparticles toward M cells by charge interactions with an electrostatic force gradient. We hypothesize that a greater surface area of clustered M cells will allow more bacteria to adhere to the apical surface and, in time, be transcytosed across the epithelium.

We looked at how groups of GFP-labeled *Staphylococcus aureus* (*S. aureus*) surround villous tips covered with M cells (Figure 4.10). We planned to use a variety of bacteria and microparticles ranging in size and charge which began with *S. aureus.* The PBS treated (control) mice showed fewer M cells and fewer adhered bacteria (Figure 4.10 A) than CT-induced villous M cell clusters (Figure 4.10 B). Clusters, induced in the CT samples, displayed M cells lining the entire villous tip, which were not able to be seen in the top-down view of the SEM images. Bacteria near the CT-induced M cell clusters were found clumped in large groups, some containing hundreds of bacteria. These larger bacteria foci were preferentially located near villous tips with large M cell clusters as opposed to villous tips with isolated single M cells. Co-localization of GFP-labeled *S. aureus* with M cells suggests the M cell clusters allow for increased sampling area and potential antigen uptake and processing. Quantification of the amount of GFP-labeled *S. aureus* adhered to a specific length of M cells in both untreated and CT-treated conditions

is provided in Figure 4.11. Quantitative data determined CT-induced M cell clusters contained larger amounts of adhered bacteria per 100 µm compared to isolated M cells and enterocytes in CT and control conditions. These results suggest that induced M cells provide less repulsive force for bacterial adhesion and sample greater amounts of bacteria than isolated M cells.

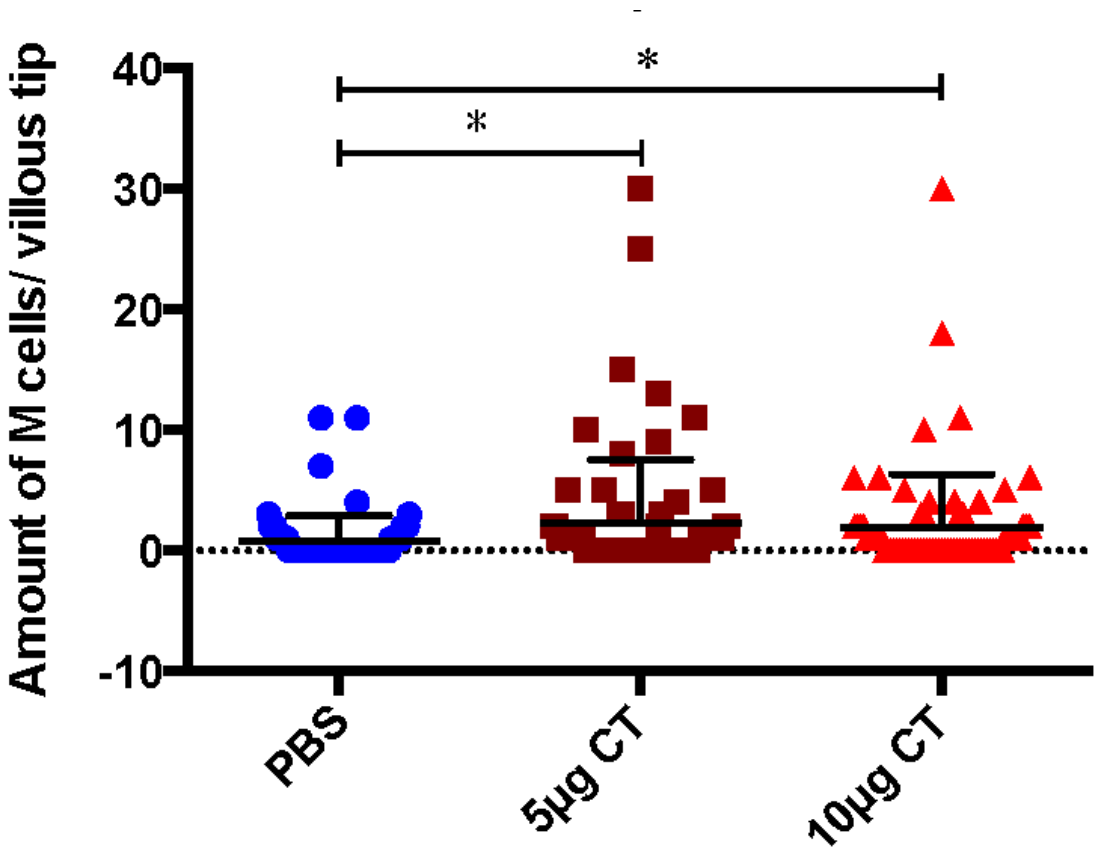

Figure 4.1 Dose optimization of CT by IP administration of 5 µg or 10 µg. Experiments had an n = 3. P-value of 5 µg dose was 0.0223 (*) whereas the 10 µg dose was 0.0485 (*) for 25 villous tips. Data was assessed using an unpaired t-test with Mann-Whitney conditions. There was a greater significance with the 5 µg dose however, there was greater amounts of M cells in one mouse of this cohort compared to the other two mice. The 10 µg dose mice had less variability of M cells across the cohort making it the optimal dose to use.

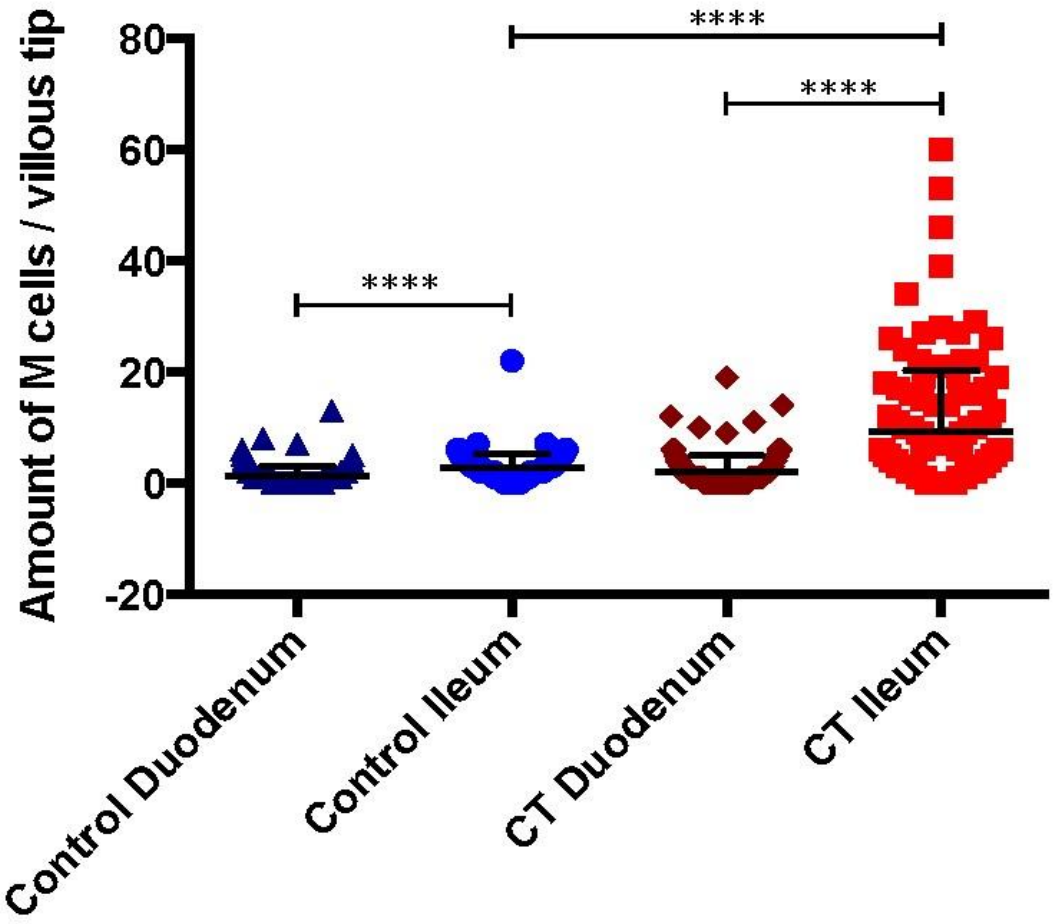

Figure 4.2 M cells counts in the duodenum and ileum of CT and control mice. Scanning electron images were quantified to determine M cell populations on 40 villi per section of the small intestine for each mouse (n = 3). P-values correspond to 0.0001 (****) and data was assessed using an unpaired t-test with Mann-Whitney conditions. Significantly higher amounts of M cells are found in the ileum over the duodenum in the control conditions. The induction of M cells, by CT, is only significant in the ileum meaning there is no significant change in M cell populations of the duodenum control verses CT-treated mice.

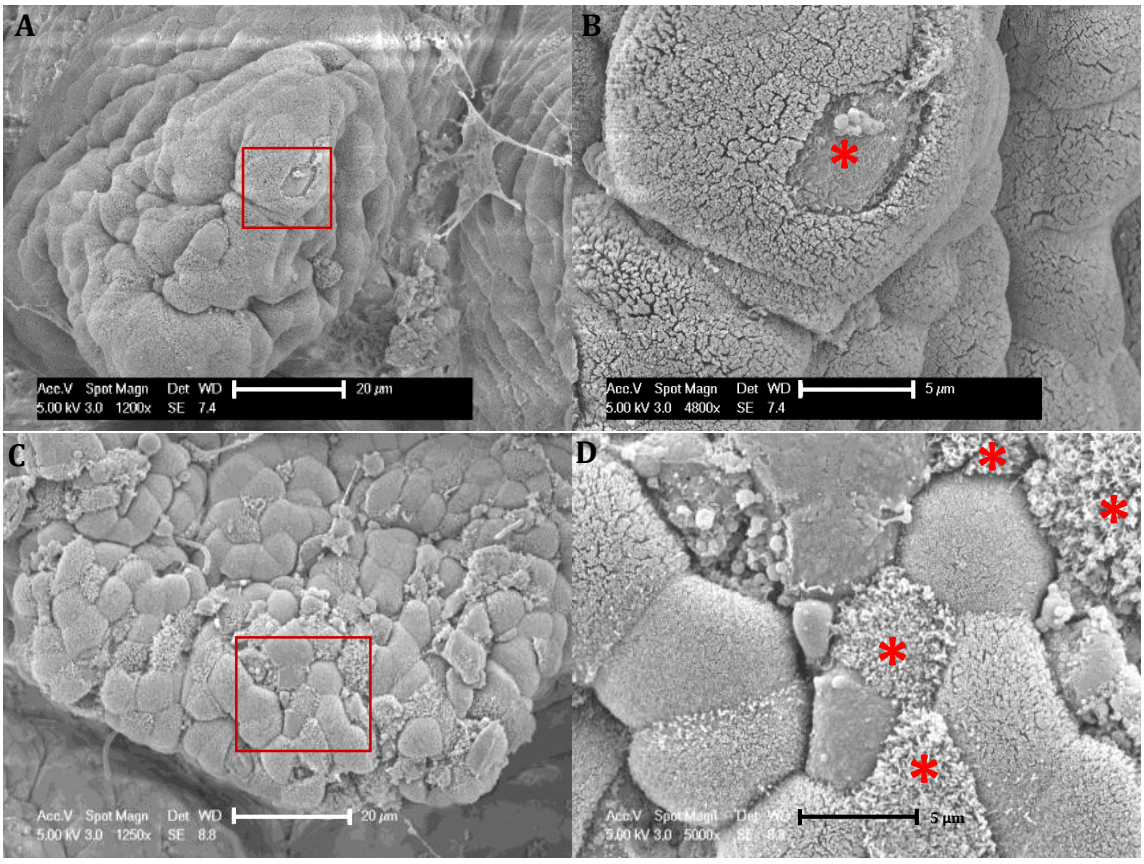

Figure 4.3 Scanning electron microscopy (SEM) images of M cells in the ileum of control and CT-treated animals. The control ileum is seen in image A and B while the CT-treated is shown in C and D. Left images (A and C) represent an image of the entire villous tip. The red box around the area of interest is magnified in images on the right (B and D). M cells are denoted with a red star in the magnified images. Left images of the villi are taken at approximately 1200x magnification where the scale bare is 20 µm (A and C) and the magnified images are approximately 5000x magnification with a scale bar of 5 µm (B and D). The induction of M cells is clearly seen here in these villi of the ileum where the control villi has one M cell and the CT-treated was counted to have over 25 M cells.

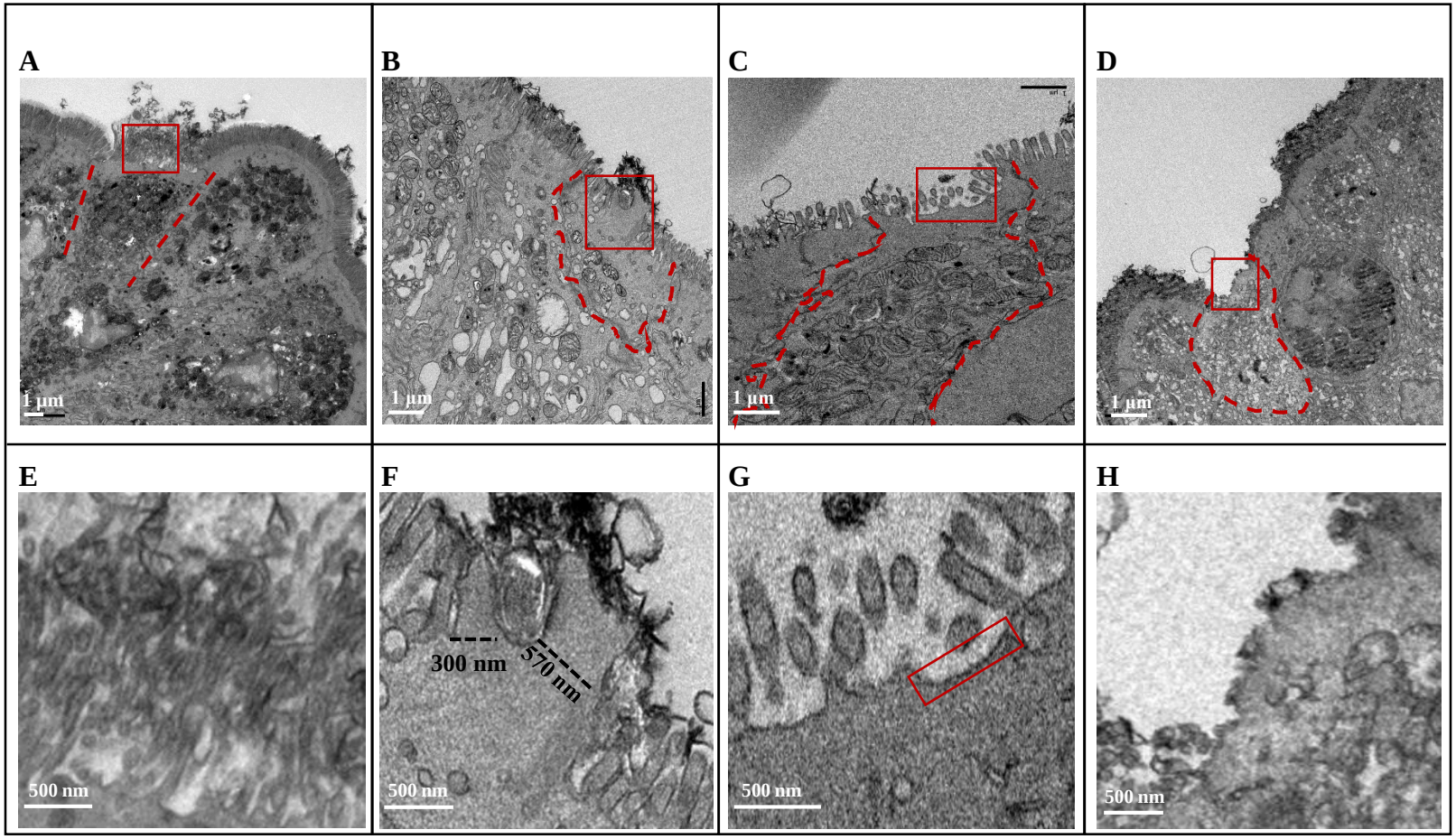
A
1 µm
B
1 µm
C
1 µm
D
1 µm
E
500 nm
F
300 nm
570 nm
500 nm
G
500 nm
H
500 nm

Figure 4.4 Transmission electron microscopy (TEM) images of control and CT-induced villous M cells. Phenotypes are of (A) disorganized microvilli M cells, (B) thicker microvilli M cells, (C) half bare and half microvilli M cells, and (D) bare apical surface M cells. Cells of interest are outlined in red dashed lines (A-D) while the close up images (E-H) are denoted in the red boxes of the original images. Disorganized microvilli are noted by the inability to see the uniform upright microvilli hairs (E). Thicker microvilli is considered anything greater than the 100 nm width of microvilli, in this case the apical extensions read 300 and 570 nm (F). Cells with both bare and microvilli surfaces show areas where the microvilli extend from the surface and areas where no extensions are seen (G). The last phenotype, bare cells, display no microvilli properties and only bare surfaces. For the main images (A-D) each scale bar is 1 μm and for the magnified images (E-H) each scale bar is 500 nm with the thickness of the tissue for each image at 70 nm.

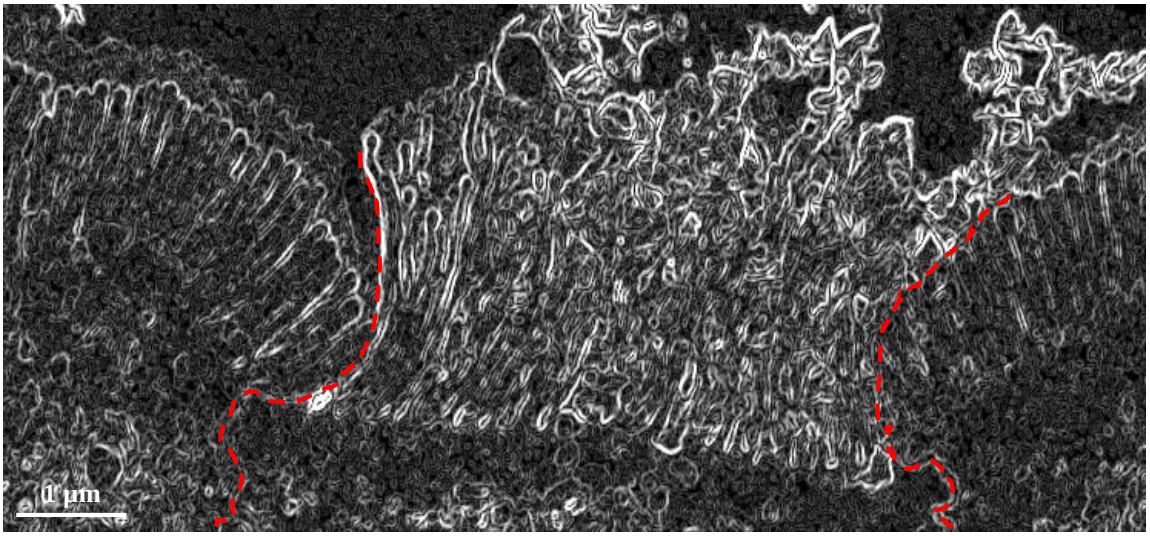

Figure 4.5 Determination of disorganized microvilli phenotype. This image distinguishes the characteristics of microvilli. The cells on the right and left surrounding the middle cell show the microvilli as organized and upright. Additionally, the microvilli are parallel to one another. The cell in the middle does not show parallel lines but appears to be more random than the standard. Red dashed lines denote the boundaries of the center cell. The image is a portion of the scanning electron microscope image from Figure 4.4 A and processed using the FIJI software tool find edges which outlines all objects in the image. Scale bar is 1 µm.

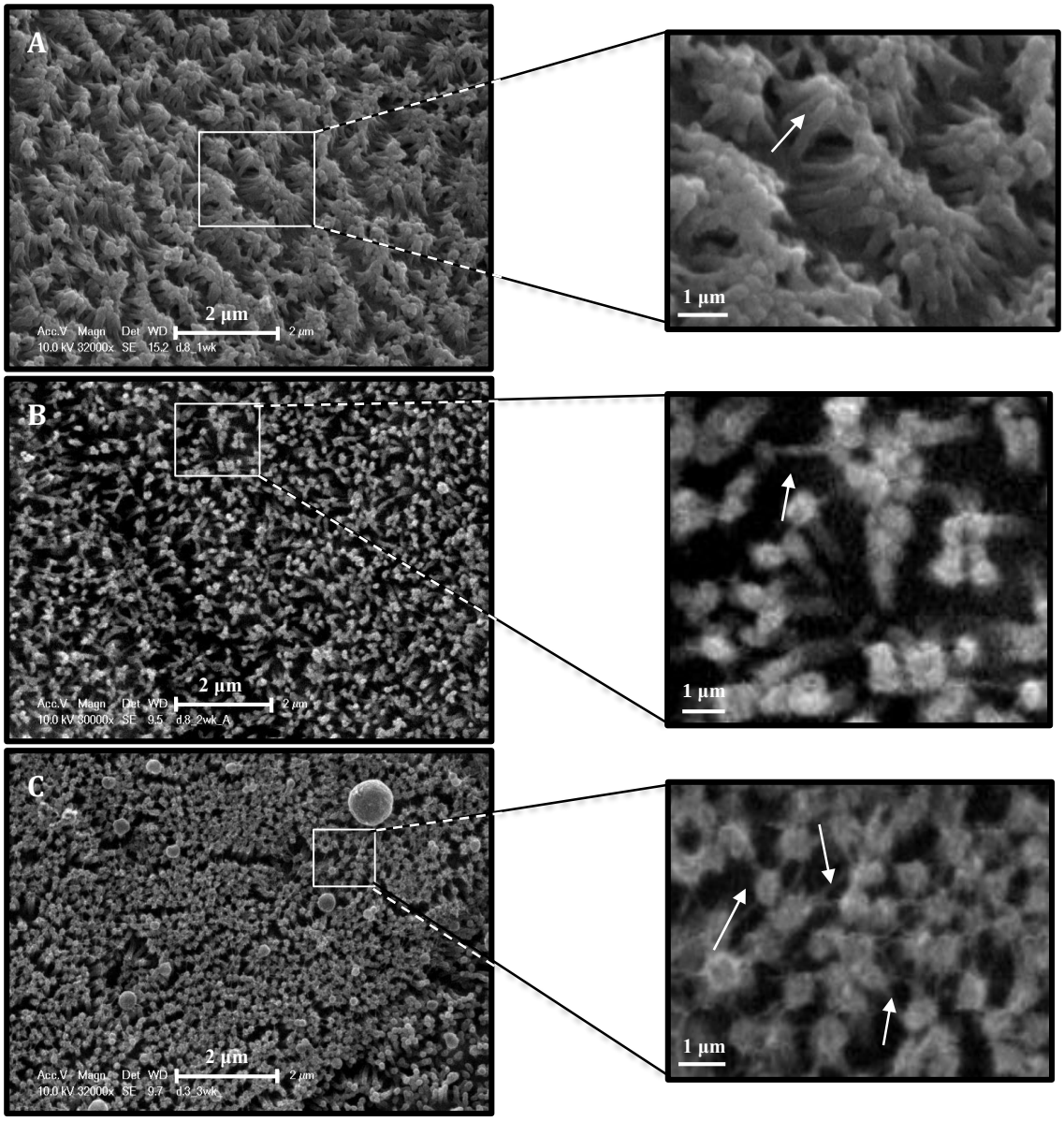
A
2 µm
Acc.V Magn Det WD
10.0 kV 32000x SE 15.2 d.8_1wk
1 µm
B
2 µm
Acc.V Magn Det WD
10.0 kV 30000x SE 9.5 d.8_2wk_A
1 µm
C
2 µm
Acc.V Magn Det WD
10.0 kV 32000x SE 9.7 d.3_3wk
1 µm

Figure 4.6 SEMs of microvilli maturation on Caco2 BBe cells at 1-week, 2-week, and 3-weeks of age. SEMs show immature stages with teepee formation (A), microvilli at an intermediate stage of maturation with neighboring microvilli pushing against each other and forming glycoprotein linkages (B), and the mature tightly packed brush border with more intermicrovillar connections of maturation with formation of an upright tightly packed brush border (C). White arrows show glycoprotein linkages connecting microvilli aiding in structural support. Right images are close ups of the boxed area on the full image on the right. Arrows represent the key features of each stage: teepees (A) and glycoprotein linkages (B and C). Scale bars represent 2 μm on the right side full image and 1 μm on the magnified image to the right.

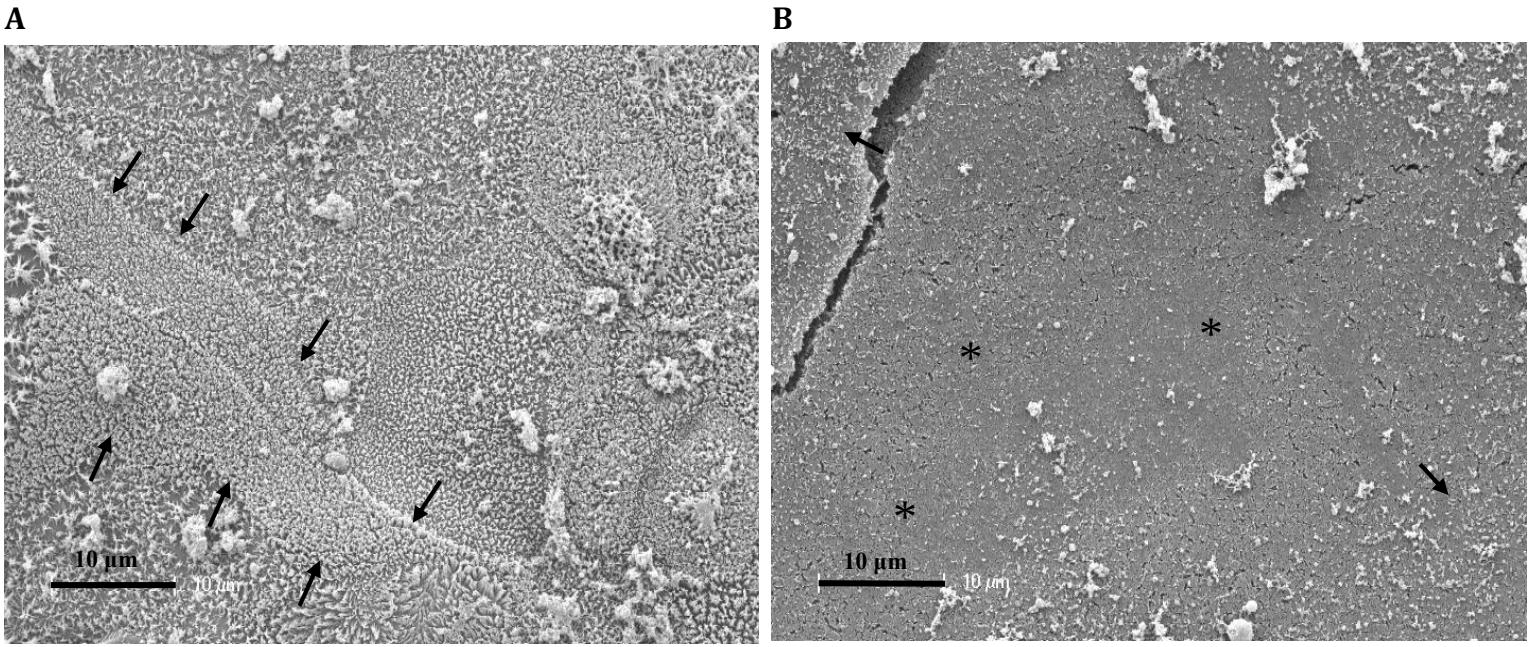

Figure 4.7 SEM images of brush border (BB) effacement in Caco2 BBe cells grown for 3 weeks. (A) Control group treated with media and (B) experimental group treated with CT for 32 hours. A mature BB is shown in the control group (A), indicated by arrows, while bare surfaces (asterisks) or shorter microvillar lengths (arrows) are seen in the CT-treated group (B). Scale bars represent 10 µm in each image.

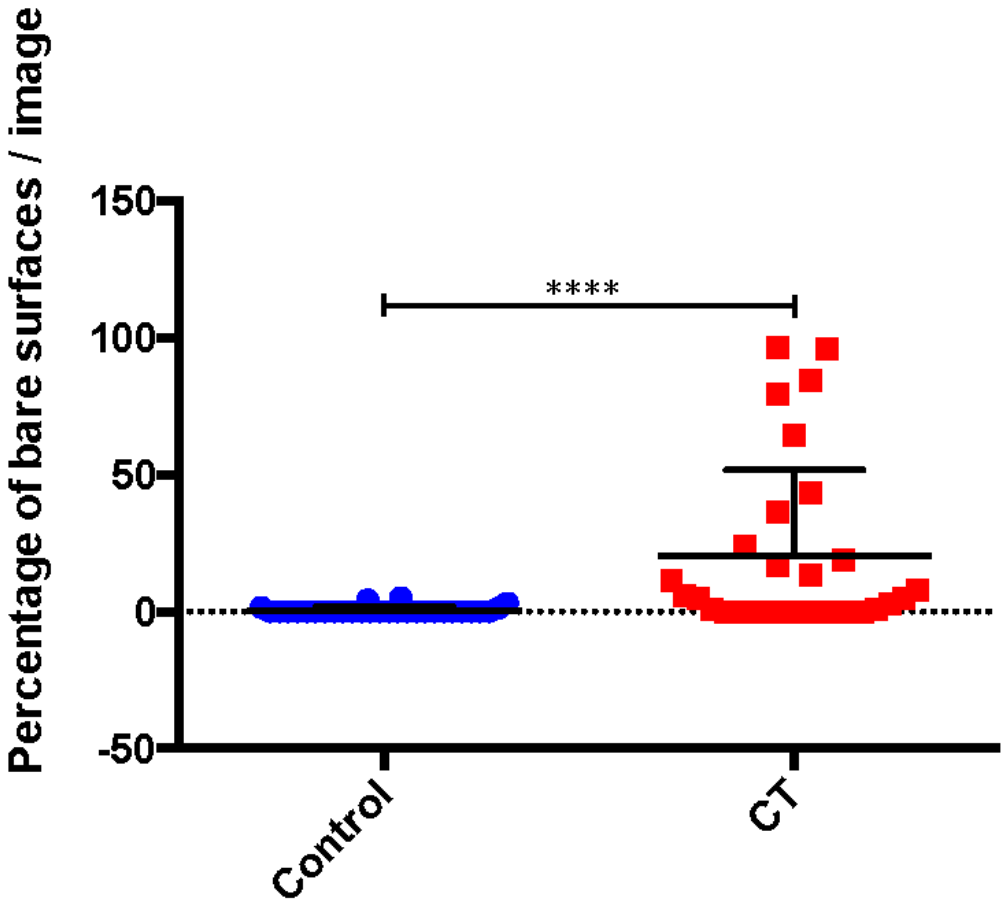

Figure 4.8 Percentage of bare surfaces in Caco2 BBe cultures treated with CT for 32 hours. Microvilli effacement is significant in CT-treated cultures. (****) is representative of a p-value < 0.0001. Data was assessed using the unpaired t-test. Three cell dishes were seeded per treatment (n = 3) and 10 SEM images were taken per dish. Cell areas were measured using FIJI software while any obstruction areas or artifacts of the SEM imaging were subtracted from the cell area. Bare areas were measured using FIJI and the percentage bare surfaces was calculated per image.

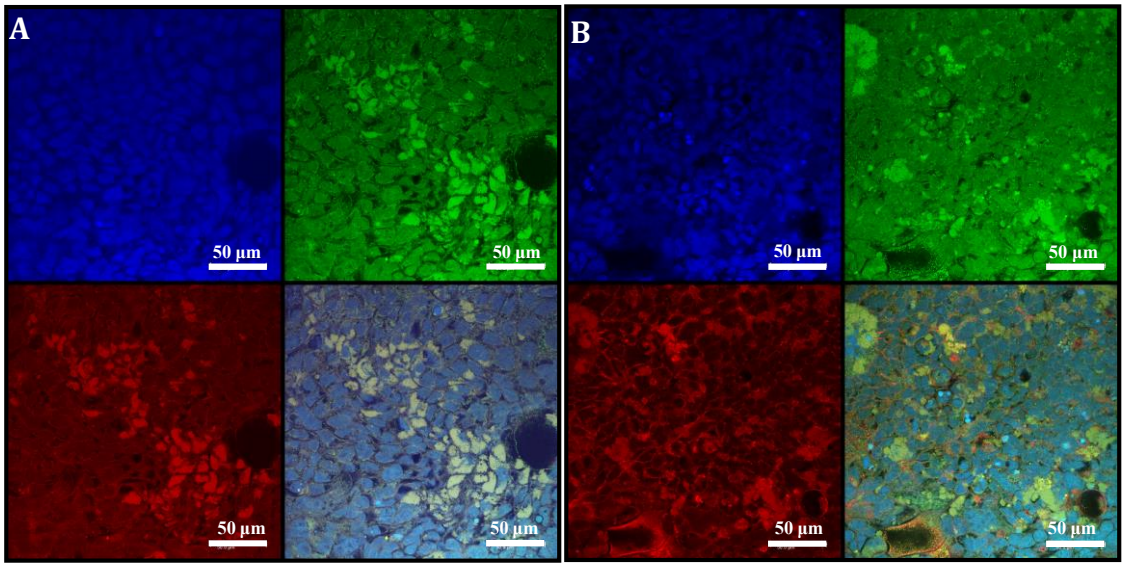

Figure 4.9 Apical PCDH24 in Caco2 BBe after CT administration. CT effaces the BB without affecting microvilli linking glycoprotein PCDH24. The control sample (A) and the CT-treated sample (B) show PCDH24 distribution. The nuclei (blue), PCDH24 (green), actin (red), and a merge channel of the 3 channels are shown. There is co-localization of the green and red channels in the merge image and is displayed in yellow. Images were taken with a 25x objective and each scale bar is 50 µm. Due to the apical surfaces being in different planes, images were taken at a plane where the majority of actin and PCDH24 was distributed throughout the image area.

A

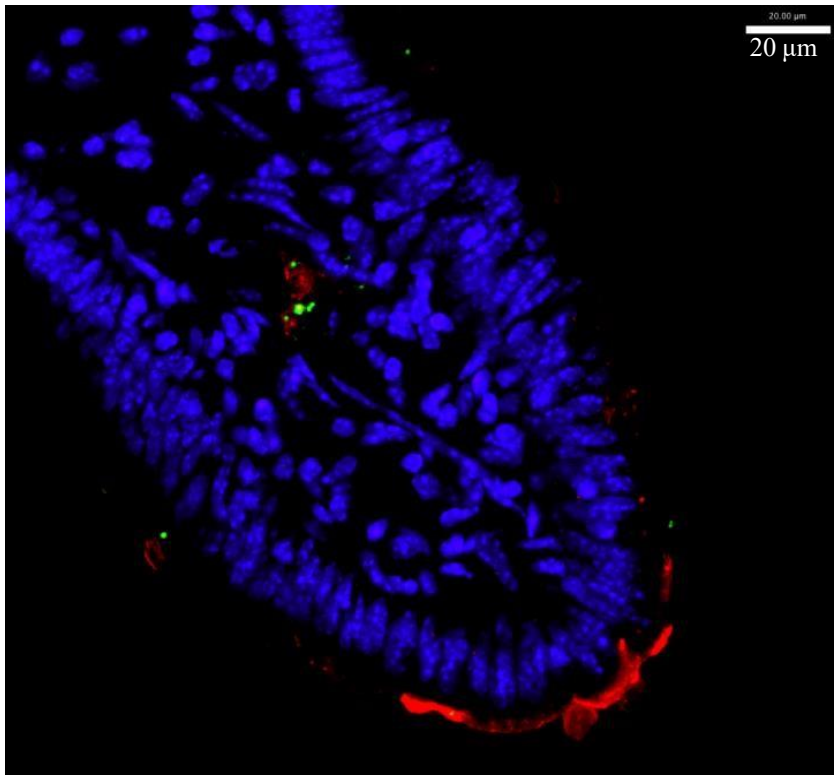

UEA-1 (M cells) DAPI (nuclei) GFP-*S. aureus*

B

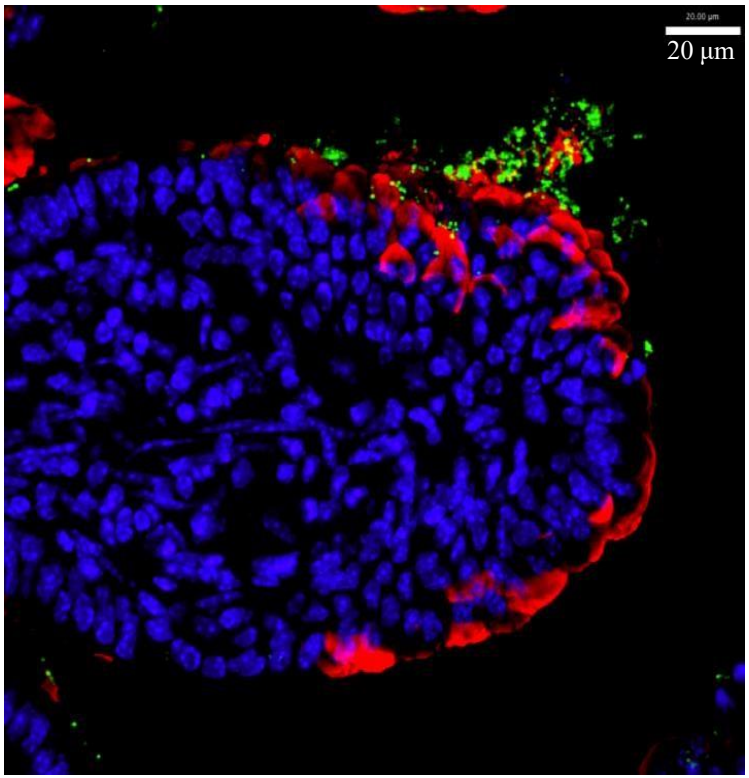

UEA-1 (M cells) DAPI (nuclei) GFP-*S. aureus*

Figure 4.10 Bacterial adhesion to villous M cells on a single villus. Fluorescent images of GFP-labeled *S. aureus* interaction with (A) control M cells and (B) CT-treated M cell clusters. M cells are stained with rhodamine conjugated UEA-1 (red), *S. aureus* is GFP-labeled (green) and nuclei are stained with DAPI (blue). Bacteria adhered to M cells display overlapping between the green and red channels as shown in yellow. Scale bars of each image is 20 μm. Fewer GFP^+ *S. aureus* are bound to M cells in the control and greater amounts are bound to M cells in CT treated samples. GFP^+ *S. aureus* form foci of bacteria in CT samples where M cell clusters are abundant, whereas isolated bacteria are seen in control samples.

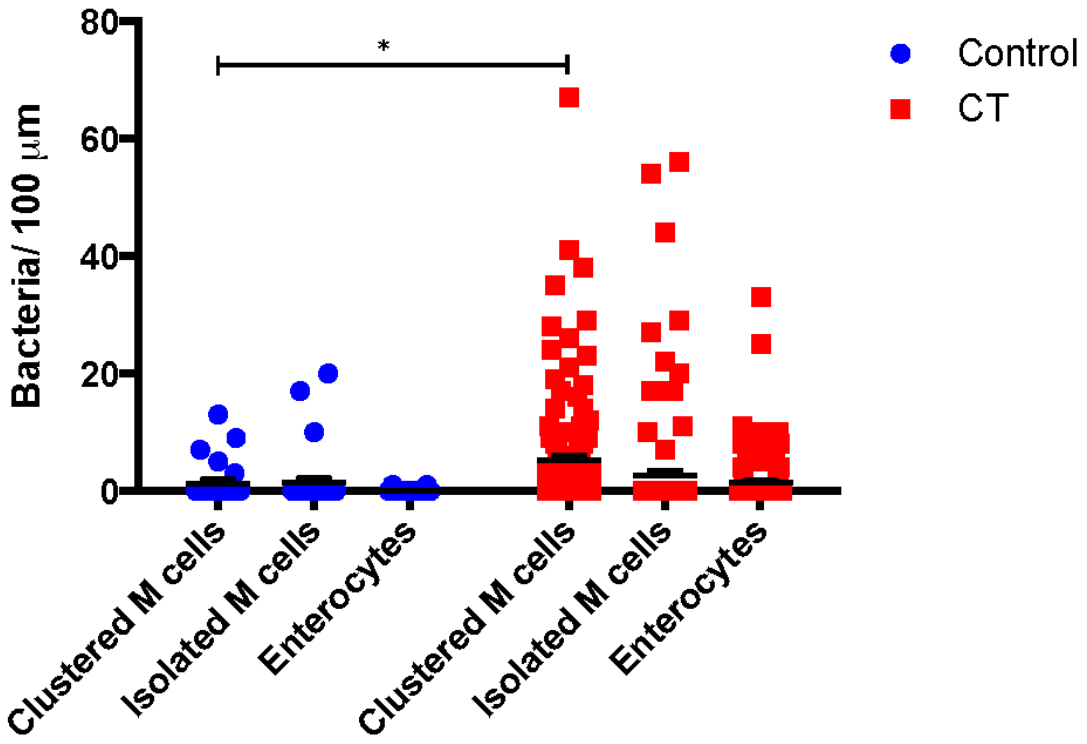

Figure 4.11 Quantification of bacterial adhesion to ileal villi. A higher number of bacteria bind to CT-induced M cell clusters than CT isolated M cells. Bacteria per 100 μm length of clustered M cells, isolated M cells, and enterocytes was analyzed in both control and CT treated groups. Bacteria per 100 μm of CT clustered M cells compared to control clustered M cells was found significant with a p-value of 0.0485. Data was assessed using an unpaired t-test.

Chapter 4 – Discussion

In this thesis we have discussed and characterized the effects of CT during physiological and controlled conditions of epithelial cells. We analyzed doses and effects of the toxin on epithelial cells, changes in endogenous cell populations, phenotypes and characteristics of cell morphology, and host-pathogens interactions. We have established *in vivo* experiments using mice, due to their similarities to humans in M cell properties, anatomy and disease pathogenesis, allowing possible extrapolation for human physiological reactions and responses to CT. Although some differences should be noted (disease symptoms, cell receptors), the mouse model is inexpensive, time efficient, relatable and provides a simple, yet relevant, non-human animal model to carry out experiments.

During the 48 hour incubation time of the toxin in the body we have determined a connection between cell, bacteria adherence and ileal-specific location of these effects. Others have demonstrated key differences in the three sections of the small intestine. One of these includes the intestinal microbiome, which may affect cell properties, function, or immune response. Significantly higher bacterial populations and species of bacteria are naturally found in the ileum compared to the duodenum, with even greater amounts in the colon. Segmented filamentous bacteria (SFB) are commensal bacteria that are known to be located exclusively in the ileum and increase immune and inflammation responses and protection (Ivanov et al. 2009, Ivanov et al. 2010). Other characteristics of the ileum

include a more neutral pH and greater amounts of mucus produced by the higher population of goblet cells. We speculate that the higher population of M cells present in the ileum is proportionally related to the change in gut microbiota, pH, and mucus. We know greater amounts of mucus correlate with the greater microbiome populations and this may suggest the need for increased antigen sampling. pH also identifies a reason for increase microbiome where different species can thrive in acidic to basic pHs, which, taken together, leads to the reason for M cell populations.

Cell morphology results from changes in physical properties, development, and behavior that may vary with changes in gene expression or environmental factors. During our studies, we have identified four apical phenotypes of epithelial cells which differ from the conventional enterocyte and M cell. As stated previously, an important difference between enterocytes and M cells is the organized mature microvilli of the enterocyte brush border (averaging 1 μm in height and 100 nm in diameter), while M cells exhibit the absence of these microvilli or contain thicker microfolds. In cases where the environment is altered, for example in disease models, microvilli have been seen to break their uniform upright positioning to adopt a collapsed position. One of our four phenotypes, M cells with disorganized microvilli, features the collapsing microvilli, and can be a result of change in gene expression which simulates PCDH24-deficient enterocytes (Crawley et al. 2014). Gene expression changes could also explain the cells with mixed characteristics, bare and thicker microvilli. It was suggested that changes in environment due to fasting or increase in vitamins or mineral uptake respectively lengthen or shorten the length of microvilli (Wasserman et al. 1983; Misch et al. 1980). A possible explanation for the variance of

phenotypes and cell amounts per phenotype from the control to CT-exposed subjects may be derived from the environmental or genetic changes caused by the toxin. Lastly, bare M cells lack microvilli and may allow more interaction with bacteria. This can be hypothesized from Bennett et al. (2014) where microvilli-absent cells have higher rates of bacteria adherence than enterocytes. The various M cell phenotypes found in CT-treated mice suggest that CT may be causing enterocytes to act like/transdifferentiate into M cells, which was also suggested in Wang et al. (2011).

Another potential explanation for the development for these phenotypes is through transdifferentiation. Our research suggests transdifferentiation is a possible contributor to M cell induction because induction is seen 48 hours post-CT administration. Transdifferentiation is the process of cells changing from one type to another without dedifferentiation back to their progenitor origin. Mach et al. (2005) suggested M cell transdifferentiation can occur either from existing enterocytes or differentiation from undifferentiated precursor cells. Pre cursor cells have been shown to form by interaction of mutant ligands with Notch (Hsieh et al. 2012; Mach et al. 2005). It could be hypothesized that Notch signaling is higher in CT-treated mice over control, but this would need to be tested.

Both *in vivo* and *in vitro* experiments demonstrate microvilli effacement, which can be derived from changes indirectly from gene expression or depletion of structures from direct action of CT as an effector molecule. Our studies suggest the effacement of the microvilli does not involve depletion of the structural transmembrane glycoprotein link

PCDH24. Microvilli effacement can happen in several ways: (1) an effector molecule can destroy the glycoprotein linkages causing folding over of the microvilli (In et al. 2016), (2) inhibition of microvillar proteins synthesis (Lecount et al. 1972) or (3) deletion or disruption of EPI64-ezrin binding complex (Hanono et al. 2006; Bennett et al. 2014). Microvilli are composed of actin filaments and crosslinking proteins ezrin, fimbrin, myosin-1, and villin. As the cell develops into an enterocyte the microvilli form and mature (Figure 4.6) During early stages, microvilli contain actin, ezrin and very little villin; however, during maturation there are greater amounts of the latter in addition to fimbrin and myosin-1 (Fath et al. 1995). It would be informative to examine the relationship between CT and the various protein compositions in the four apical phenotypes of treated and control cells. Based off our *in vitro* and *in vivo* experiments with M cell phenotypes and microvilli effacement, we hypothesize there is a significantly greater amount of fimbrin and myosin in the control than in the CT-treated cells. That being said, the effacement, transdifferentiation, or phenotypic occurrences could alternatively be derived from changes in gene expression caused by the toxin.

Finally, we analyzed adherence rates of bacteria on isolated and clustered M cells in control and CT-treated conditions. We had noticeably greater amounts of bacterial adherence in CT-treated mice over control conditions and bacteria formed clusters. Pathogenic bacteria are known to invade an area of interest by forming clusters or biofilms with other bacteria. Since it is suggested (Atuma et al. 2001) that mucus rids the body of pathogenic bacteria by capturing a single bacterium into the mucus glycocalyx matrix and carrying it away, it is more difficult to entrap and remove clusters of bacteria or biofilms.

Therefore, we can propose that in the CT-treated condition, where M cell clusters are more prominent, bacteria preferentially cluster in order to more easily penetrate the mucus to reach the epithelium. With this new idea posed, it would be vital to determine if the greater area of M cell clusters during CT exposure is an effect produced by the toxin to make invasion more efficient. To understand the function of these induced M cells, it is necessary to conduct transcytosis assays to determine what percentage of bacteria that is transported across the epithelium or if these M cells trap the bacteria on the apical surface for easy disposal.

Chapter 5 – Conclusion

M cell clusters on villi are induced upon treatment with CT and they range anywhere from two M cells to 50 or more M cells. These clusters are present at a higher number in the distal portion of the small intestine and SEM has been demonstrated to be a substantial tool in examining M cells. These large clusters could be helpful in designing therapeutic reagents targeted for antigen or vaccine delivery to M cells for transference to underlying APCs.

Secondly, we determined that M cells on the villi have a variety of phenotypes, which can be found in both control and CT-treated M cell clusters. It would be interesting to consider how these phenotypes are affected in host-pathogen interactions, antigen uptake and recognition, and cell communication based on electrostatic interactions. We are aware from previous studies that there is a difference in electrostatic potential between enterocytes and M cells. Perhaps these four M cell phenotypes have different electrostatic potentials based on their apical phenotype. For instance, the phenotype that represents a completely bare apical surface would have a more neutral surface charge compared to the disorganized M cell phenotype, which would have a more negative surface charge. Bacteria species differ in their charge and adherence to more neutral surfaces, dependent on their electrostatic potential (Bennett et al. 2014). We could hypothesize that these phenotypes have differential adherence rates depending on bacterial charge. Since *S. aureus* displays a highly negative charge it would more readily adhere to phenotypes with little to no microvilli than bacteria with a less negative charge such as *S. typhimurium.* These different

phenotypes could allow M cells to sample different species of bacteria or would allow more bacteria to colonize. It should also be determined if these phenotypical changes arise from changes in gene expression or post-translational modifications. For the microvilli phenotypes, further analysis can be conducted in cell cultures with CT using cross sections in TEM which may give similar phenotypes as seen *in vivo*. These cell cultures can then be analyzed with a microarray to look at changes in gene expression.

We determined that exposure to CT can result in morphological changes to the Caco2 BBe cells, causing their microvilli to shorten or be lost. We tested how CT was able to remodel the microvilli by looking at PCDH24, the structural component creating an upright BB. We found that CT does not affect the glycoprotein linkages in microvilli, and has been reported in the presence of some drugs, which decreases the height and width of the microvilli, but does not affect its upright structure (Lecount et al. 1972). Elucidating the protein composition of microvilli would provide great insight into understanding microvilli biology in physiological and disease states. The CT may be inhibiting the synthesis of microvilli-associated proteins required for microvilli to maintain their length and stability (Stidwell et al. 1984).

Lastly, we looked into functional properties of these M cell clusters with GFP-labeled *S. aureus*. *S. aureus* adherence to M cells was increased in CT-treated animals. Since CT-induced M cell clusters are larger in size, this may allow for a greater surface area for increased uptake and immunosurveillance. Understanding the functional properties and interactions of induced M cells provides more information on host pathogen interactions. If these induced M cells clusters are attracting more bacteria than isolated M

cells, this may mean there is a greater electrostatic potential between enterocytes and M cell clusters versus isolated M cells. This observation may also be due to immune system attempting to better survey antigens or control the course of an infection or disease. Alternatively, the bacteria may be inducing M cell clusters for their benefit by making the intestinal microenvironment more habitable. Future studies could take advantage of this cluster forming property by designing drugs to induce M cell clusters that would increase immune surveillance and result in a beneficial disease outcome.

Chapter 6 – References

Atuma, C., Strugala, V., Allen, A., Holm, L. (2001). The adherent gastrointestinal mucus gel layer: thickness and physical state in vivo. *American Journal of Physiology-Gastrointestinal and Liver Physiology*,*280*(5), G922-G929.

Bennett, K. M., Parnell, E. A., Sanscartier, C., Parks, S., Chen, G., Nair, M. G., Lo, D. D. (2016). Induction of Colonic M Cells during Intestinal Inflammation. *The American journal of pathology*, *186*(5), 1166-1179.

Bennett, K. M., Walker, S. L., Lo, D. D. (2014). Epithelial microvilli establish an electrostatic barrier to microbial adhesion. *Infection and immunity*, *82*(7), 2860-2871.

Borghesi, C., Taussig, M. J., Nicoletti, C. (1999). Rapid appearance of M cells after microbial challenge is restricted at the periphery of the follicle-associated epithelium of Peyer's patch. *Laboratory investigation; a journal of technical methods and pathology*, *79*(11), 1393-1401.

Clark, M. A., Jepson, M. A., Simmons, N. L., Booth, T. A., Hirst, B. H. (1993). Differential expression of lectin-binding sites defines mouse intestinal M-cells. *Journal of Histochemistry & Cytochemistry*, *41*(11), 1679-1687.

Crawley, S. W., Shifrin, D. A., Jr., Grega-Larson, N. E., McConnell, R. E., Benesh, A. E., Mao, S., Zheng, Y., Zheng, Q. Y., Nam, K. T., Millis, B. A., Kachar, B., Tyska, M. J. (2014) Intestinal brush border assembly driven by protocadherin-based intermicrovillar adhesion. *Cell* 157, 433-46.

Creamer, B. (1967) The turnover of the epithelium of the small intestine. *British medical bulletin* 23, 226-30.

Evans, D. F., Pye, G., Bramley, R., Clark, A. G., Dyson, T. J., Hardcastle, J. D. (1988) Measurement of gastrointestinal pH profiles in normal ambulant human subjects. *Gut* 29, 1035-41.

Fath, K. R., Burgess, D. R. (1995). Microvillus assembly: not actin alone. *Current Biology*, *5*(6), 591-593.

Guichard, A., Cruz-Moreno, B., Aguilar, B., van Sorge, N. M., Kuang, J., Kurkciyan, A. A., Wang, Z., Hang, S., Pineton de Chambrun, G. P., McCole, D. F., Watnick, P., Nizet, V., Bier, E. (2013) Cholera toxin disrupts barrier function by inhibiting exocyst-mediated trafficking of host proteins to intestinal cell junctions. *Cell Host & Microbe* 14, 294-305.

Hanono, A., Garbett, D., Reczek, D., Chambers, D. N., Bretscher, A. (2006). EPI64 regulates microvillar subdomains and structure. *The Journal of cell biology*, *175*(5), 803-813.

Hase, K., Kawano, K., Nochi, T., Pontes, G. S., Fukuda, S., Ebisawa, M., Kadokura, K., Tobe, T., Fujimura, Y., Kawano, S., Yabashi, A., Waguri, S., Nakato, G., Kimura, S., Murakami, T., Iimura, M., Hamura, K., Fukuoka, S., Lowe, A. W., Itoh, K., Kiyono, H., Ohno, H. (2009) Uptake through glycoprotein 2 of FimH(+) bacteria by M cells initiates mucosal immune response. *Nature* 462, 226-30.

Hsieh, E. H. and Lo, D. D. (2012) Jagged1 and Notch1 help edit M cell patterning in Peyer's patch follicle epithelium. *Developmental and comparative immunology* 37, 306-12.

Hsieh, E. H., Fernandez, X., Wang, J., Hamer, M., Calvillo, S., Croft, M., Kwon, B. S., Lo, D. D. (2010) CD137 is required for M cell functional maturation but not lineage commitment. *The American Journal of Pathology* 177, 666-76.

In, J., Foulke-Abel, J., Zachos, N. C., Hansen, A. M., Kaper, J. B., Bernstein, H. D., Halushka, M., Blutt, S., Estes, M. K., Donowitz, M., Kovbasnjuk, O. (2016) Enterohemorrhagic reduce mucus and intermicrovillar bridges in human stem cell-derived colonoids. *CMGH Cellular and Molecular Gastroenterology and Hepatology* 2, 48-62 e3.

Ivanov, II and Littman, D. R. (2010) Segmented filamentous bacteria take the stage. *Mucosal Immunology* 3, 209-12.

Ivanov, II, Atarashi, K., Manel, N., Brodie, E. L., Shima, T., Karaoz, U., Wei, D., Goldfarb, K. C., Santee, C. A., Lynch, S. V., Tanoue, T., Imaoka, A., Itoh, K., Takeda, K., Umesaki, Y., Honda, K., Littman, D. R. (2009) Induction of intestinal Th17 cells by segmented filamentous bacteria. *Cell* 139, 485-98.

Kerneis, S., Bogdanova, A., Kraehenbuhl, J. P., Pringault, E. (1997) Conversion by Peyer's patch lymphocytes of human enterocytes into M cells that transport bacteria. *Science* 277, 949-52.

Lange, K. (2000) Microvillar ion channels: cytoskeletal modulation of ion fluxes. *Journal of Theoretical Bioliology* 206, 561-84.

Lecount, T. S. and Grey, R. D. (1972) Transient shortening of microvilli induced by cycloheximide in the duodenal epithelium of the chicken. *Journal of Cell Biology* 53, 601-5.

Lelouard, H., Fallet, M., de Bovis, B., Meresse, S., Gorvel, J. P. (2012) Peyer's patch dendritic cells sample antigens by extending dendrites through M cell-specific transcellular pores. *Gastroenterology* 142, 592-601 e3.

Lencer, W. I. (2001) Microbes and microbial Toxins: paradigms for microbial-mucosal toxins. V. Cholera: invasion of the intestinal epithelial barrier by a stably folded protein toxin. *American Journal of Physiology. Gastrointestinal and Liver Physiology* 280, G781-6.

Mach, J., Hshieh, T., Hsieh, D., Grubbs, N., Chervonsky, A. (2005). Development of intestinal M cells. *Immunological reviews*, *206*(1), 177-189.

Meynell, H. M., Thomas, N. W., James, P. S., Holland, J., Taussig, M. J., Nicoletti, C. (1999). Up-regulation of microsphere transport across the follicle-associated epithelium of Peyer's patch by exposure to Streptococcus pneumoniae R36a. *The FASEB journal*, *13*(6), 611-619.

Misch, D. W., Giebel, P. E., Faust, R. G. (1980). Intestinal microvilli: responses to feeding and fasting. *European Journal of Cell Biology*, *21*(3), 269-279.

Rescigno, M., Urbano, M., Valzasina, B., Francolini, M., Rotta, G., Bonasio, R., Granucci, F., Kraehenbuhl, J. P., Ricciardi-Castagnoli, P. (2001) Dendritic cells express tight junction proteins and penetrate gut epithelial monolayers to sample bacteria. *Nature Immunology* 2, 3617.

Savidge, T. C., Smith, M. W., James, P. S., Aldred, P. (1991). Salmonella-induced M-cell formation in germ-free mouse Peyer's patch tissue. *The American journal of pathology*, *139*(1), 177.

Stidwill, R. P., Wysolmerski, T., Burgess, D. R. (1984) The brush border cytoskeleton is not static: in vivo turnover of proteins. *The Journal of Cell Biology* 98, 641-5.

Wang, J., Gusti, V., Saraswati, A., Lo, D. D. (2011) Convergent and divergent development among M cell lineages in mouse mucosal epithelium. *The Journal of Immunology* 187, 5277-85.

Wasserman, R. H., and Fullmer, C. S. (1983). Calcium transport proteins, calcium absorption, and vitamin D. *Annual Review of Physiology*, *45*(1), 375-390.